Damage in Composite NiMH Positive Electrodes

A. M. Sastry

S. B. Choi

X. Cheng

Department of Mechanical Engineering,
and Applied Mechanics
The University of Michigan,
Ann Arbor, MI 48109-2125

Mechanical degradation in fibrous composite electrodes in use in NiMH (nickel metal hydride) batteries is being studied. NiMH cells exhibit failure in the positive plate due to swelling induced during the electrochemical reaction, which leads to gradual breakdown of the connectivity of the substrate microstructure. Particularly, loss of electrical conductivity as related to losses in mechanical properties upon cell cycling (constant current cycles with substantial overcharge) are being investigated experimentally. These properties are measured for the dry substrate material before and after battery cycling, and the losses observed suggest key failure mechanisms including mechanical damage. Results suggest tradeoffs between use of higher density nickel substrates and improved energy densities using mechanical and resistivity proof tests.

I Introduction: Mechanical Damage in NiMH Battery Electrodes

NiMH (nickel metal-hydride) battery technology has been greatly advanced through use of improved materials. In vehicle applications, both high power (hybrid electric vehicles, or HEVs) and high storage capacity (electric vehicles, or EVs) cells are desirable. Importantly, the energy density of these cells determines their cost-effectiveness.

The positive plate in the NiMH cell is comprised of a substrate of a porous nickel material; this positive electrode is the same as that in a NiCd (nickel-cadmium) cell. Figure 1 shows some of their microstructures schematically. Technology has progressed from sintered nickel plates, to nickel foams, to fibrous architectures (Fritts, 1981; Ettel, 1994, 1993; Sastry, 1994). The porous nickel substrate is impregnated with active material (Fig. 2), to form the positive plate, then immersed in electrolyte with a negative plate to form the cell. Each of the successive substrate technologies in Fig. 1 has demonstrated improved capacity with lower density, reducing the cell weight. One key failure mode in the NiMH cell arises from loss of electrical conductivity in the positive plate due to electrochemically-induced swelling. Use of advanced, lower density microstructures (usually fibrous) in the positive plate generally exacerbates the problem of swelling. Formation of the γ-NiOOH phase (primarily upon overcharge), which is of lower density than the β-Ni$(OH)_2$, leads to fatigue upon charge/discharge cycles of the electrodes, which limits their performance (Fritts, 1981; Oshitani et al., 1986, who studied NiCd cells). Work has been done to reduce the formation of the γ-phase in the positive plate; additives such as cobalt (ibid.) have shown some success, but at substantial materials cost. Solutions to this difficulty include compression of the cell casing to control swelling, presumably providing better conductivity and performance of the positive plate, through improved contact between active material and substrate. Since these cells are positive plate-limited in capacity, improved positive electrodes are of critical importance.

II Experimental Methodology

The present study was focused on assessing the mechanical damage induced in fibrous networks in NiMH cells. Concurrent experiments were performed to assess conductivity losses in the substrates, which were postulated to be related to connectivity changes in the material due to mechanical damage. Substrate materials were assessed with image analysis, and then characterized for conductivity (resistivity) and mechanical properties before and after cycling. The substrates alone i.e., the unfilled, fibrous networks, were tested in all cases. "Electrode" or "plate" in the current investigation refers to the substrate loaded, or filled with active material. This active material was removed for post-cycling testing of the substrates.

Materials. The positive plates in this study were comprised of fibrous/particulate composite substrates impregnated with active material. The active material used was produced by Tanaka, and consisted of 88.7% NiOH, 5% Co, 6% CoO, and 0.3% PVA, by weight. Table 1 gives the composition of the substrate materials investigated. These materials were produced by National Standard. Image analysis was performed on the materials, to characterize their microstructure. All were found to have roughly uniformly distributed orientations of fibers, in-plane and out-of-plane. For the post-cycled materials, three cells of each material type were constructed and cycled; three small specimens from each material type were tested for both mechanical properties and resistivity.

Cell Experimentation

Cell Composition. The cells in this study were comprised of three electrodes; one positive and two negative plates ("tri-electrodes"). The negative (metal) plates used were produced by Ovonic, and contained an expanded metal grid to ensure adequate conductivity. The electrolyte used was a solution of 30% KOH weight plus 1.5% weight of LiOH.

The cells formed in this study had capacities ranging from approximately 0.2–0.6 Ah. The electrodes were sealed in separator bags and inserted between two Plexiglas test blocks, measuring 0.5 in. (1.27 cm) thick and ranging from 3 in. × 4 in. to 2.5 in. × 3.5 in. (7.6 × 10.2 to 6.3 × 8.9 cm), secured together by bolts in each corner to compress the electrodes.

Cell Cycling. A constant current charge/discharge regime was used to cycle the cells; this experiment is typically used to determine both the effective cell capacity and the effect of discharge rate on capacity. The test procedure was developed by the United States Advanced Battery Consortium (USABC, 1996). The cells' effective capacities were first determined with a set of four charge/discharge cycles, with an overcharge of 115 percent of theoretical capacity (determined by the cells' active weights). Cells were then cycled until either 1) 40 cycles

Contributed by the Materials Division for publication in the JOURNAL OF ENGINEERING MATERIALS AND TECHNOLOGY. Manuscript received by the Materials Division September 18, 1997; revised manuscript received February 9, 1998. Associate Technical Editor: D. Allen.

Copyright © 1998 by ASME

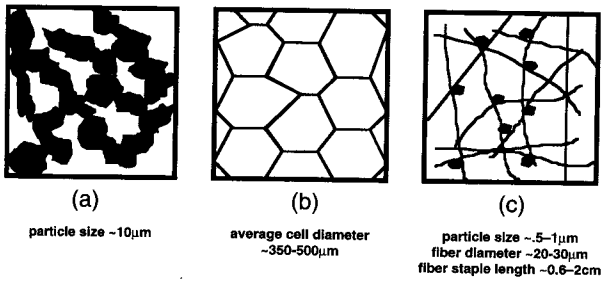

Fig. 1 Progression of NiMH positive plate substrate technology, from (*a*) sintered nickel plates, to (*b*) nickel foams, to (*c*) fibrous (with or without particulate nickel) substrates.

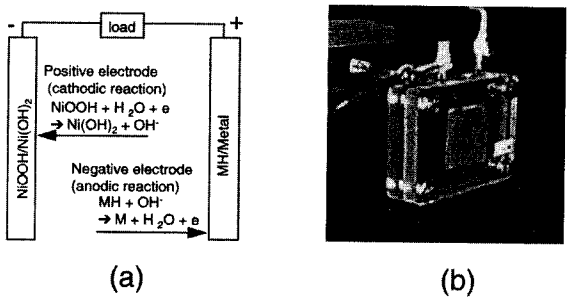

Fig. 2 Electrochemical reaction in a nickel-metal hydride cell in schematic (*a*), and a test cell (*b*) used in the current study with the positive plate comprised of a composite (fibrous) network impregnated with active material.

were reached, or 2) capacity dropped to 80 percent of initial capacity (80 percent utilization). The loss of capacity with cycle life was approximately linear, as shown in Fig. 3. Complete cycles consisted of 150 percent overcharge at a charge rate of (actual capacity)/3 hours ("C/3" rate), followed by a C/3 discharge to 0.9 V. The 150 percent overcharge value was suggested by Oshitani's work (1986) in sintered NiMH positive plates.

Figure 4 shows the charge/discharge curves for a typical trielectrode cell tested. Note that the discharge at 40 cycles to 0.9 V is complete in less time than in the first full cycle. All 40 cycles were run after the preliminary (4) cycles used to assess the cell's actual capacity. All cells tested were run in the "flooded" condition, meaning that electrolyte was added to the cells periodically to prevent cell drying. Full testing of a single tri-electrode cell in 40 cycles of constant current, C/3-rate testing (including formation and capacity-calculation cycles) required 1–2 weeks.

Plate Deloading. Post-cycling evaluation (resistivity and mechanical testing) of the positive plate substrates was performed after all of the remaining active material impregnated in the plates was chemically removed, or deloaded. The deloading was critically important, as remaining active material in the plate would have added conductive mass to the substrate, preventing assessment of loss of substrate conductivity upon cycling.

Active material was removed from the substrates by soaking at 65°C in a solution of Ammonium Hydroxide ($NH_4(OH)_2$), EDTA, distilled water and hydrazine sulfate, followed by rinsing in distilled water, and drying in a low-temperature oven (~150°C). This procedure was repeated until the active material was fully removed. In all cases, negligible loss of nickel in the substrates was measured (by comparison of pre-cycled and post-cycled substrate masses). However, image analysis revealed significant differences in connectivity and microstructural features in the two conditions. These physical changes are the subject of continued study.

Electrical Resistivity Testing. Specimens were cut directly from the substrates after deloading, as shown in Fig. 5(*a*). Uncycled substrates were first tested to determine their effective resistivity, using a Keithley model 195A digital multimeter. An eight probe apparatus was constructed for this purpose (Fig. 5(*b*)). The transport in these fibrous structures is the subject of an ongoing analytical/numerical study, and experimental validation is described in greater detail in et al. (1997a).

Materials were tested in a plane configuration, with the eight probes positioned orthogonally to the plane of the substrate, located directly across from one another in each of the four corners of the rectangular specimens. Several lengths of specimens were tested for the uncycled substrate, and their resistivities were averaged. The specimens from the cycled substrates were of the same dimensions, as shown in Fig. 5(*b*). The specimens' resistivities were first measured; then they were destructively tested for mechanical properties.

Mechanical Testing. The Young's moduli and peak stresses were measured for both materials, for cycled and uncycled conditions. The mechanical properties of this class of fibrous structures are the subject of another ongoing analytical/numerical study, described in some detail in Sastry et al. (1998). Several strain rates were initially used on the uncycled materials; little sensitivity was found, so a strain rate of ~.1 min^{-1} was used for the uncycled materials, and ~.25 min^{-1} for the cycled materials, for convenience in the separate test configurations.

Specimens for the uncycled substrates followed a protocol adapted from ASTM D 828-93 for paper and paperboard, and measured 2.25 in. × 1 in. (~5.7 cm × 2.5 cm). Specimens for the cycled substrates were limited to the size shown in Fig. 5(*a*), of 1.5 in. × 0.75 in. (~3.8 cm × 1.9 cm).

The stress-strain response of these materials exhibited a generally nonlinear behavior, as shown in Figs. 6(*a*)–(*d*). Initial (secant) moduli were computed in each case at approximately 0.2 percent strain.

III Results

Results of the mechanical and resistivity experiments are shown in Figs. 7 and 8. Moduli for the 18 and seven percent substrates dropped, by 10 and 22 percent, respectively, upon cycling, while peak stresses actually rose by 32 and 54 percent. Resistivities rose significantly, as would be expected, for the cycled substrates, by 184 and 53 percent, respectively. Thus, the higher volume fraction material (18 percent) showed a greater sensitivity to cycling with respect to final resistivity; the lower volume fraction (seven percent) showed a greater sensitivity to cycling with respect to modulus. The increase in peak stress in both cases was significant, with higher sensitivity in the lower volume fraction (seven percent) material.

IV Discussion/Future Work

The in situ loads on the substrate materials upon electrochemical cycling are complex and multiaxial. Generally, such loading

Table 1 Materials tested. Both materials were produced by National Standard

Material Type	Thickness	Content	Fiber d	Particle d	Fiber Staple Length	Vol % Nickel
Fibrex (001-008)	0.03" (0.08cm)	97% pure nickel, 3% contaminant: 50/50 blend fiber/powder	~30μm	1μm	0.25-0.5 " (~.64-1.3cm)	~18%
Fibrex (001-028)	0.08" (0.20cm)	97% pure nickel, 3% contaminant: 50/50 blend fiber/powder	~30μm	1μm	0.25-0.5" (~.64-1.3cm)	~7%

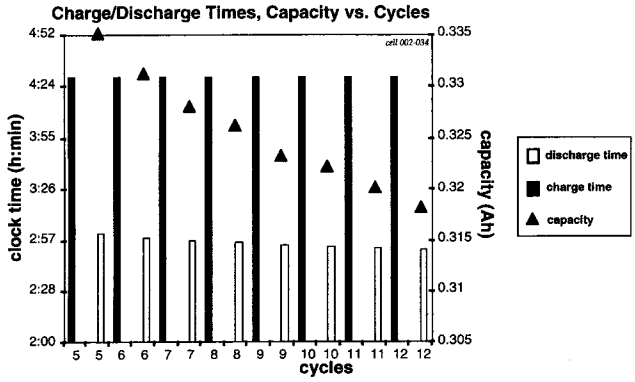

Fig. 3 Capacity loss upon cycling for a typical trielectrode cell. The charge portion of the cycle is to 150 percent of the rated capacity, and the discharge portion is to 0.9 V (nominal cell voltage: 1.25 V).

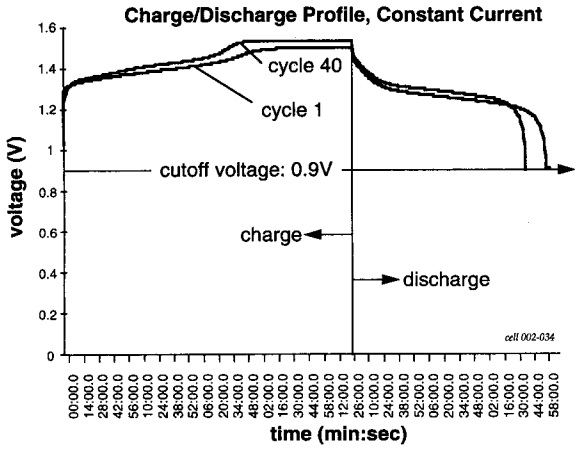

Fig. 4 Charge/discharge profile (voltage versus time) for a typical trielectrode cell. Loss in potential from the first cycle (cycle 1) to the last is shown by the two curves. Chargin/discharging were performed at a C/3 rate.

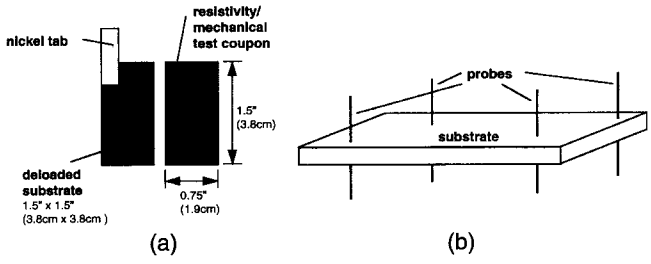

Fig. 5 Resistivity measurement schematic (*a*) and coupon from deloaded positive plate (*b*)

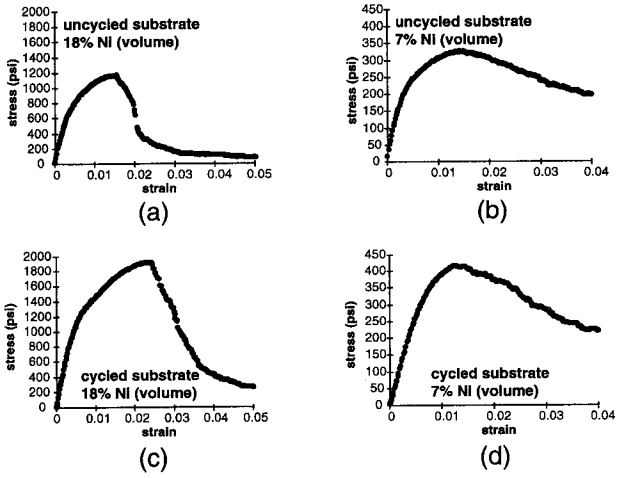

Fig. 6 Mechanical response of uncycled and cycled materials: (*a*) uncycled, 18% Ni material; (*b*) uncycled, 7% Ni material; (*c*) cycled, 18% Ni material; (*d*) cycled, 7% Ni material.

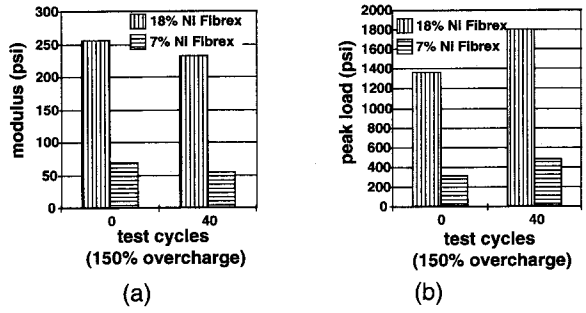

Fig. 7 Results of mechanical testing of uncycled and cycled substrate materials, including moduli (*a*) and peak stresses (*b*)

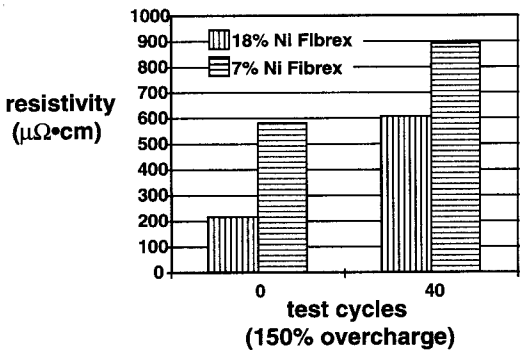

Fig. 8 Results of resistivity measurements on uncycled and cycled materials

is presumed to be hydrostatic swelling (e.g., Davolio, 1990). Amorphous fibrous structures of this type provide an excellent combination of high active surface area with low density, but local loads in these materials vary greatly (Sastry et al., 1998), and are highly dependent upon connectivity of the microstructures. It has been shown with the experiments here that breakdown in microstructural integrity of these materials can be assessed not only through application of complex loads applied in situ, but also by ex situ mechanical and transport experiments.

Loss of connectivity upon swelling of the electrode during electrochemical cycling explains much of the observed behavior. The sensitivities observed in each case suggest that materials of different construction have different "percolation points" for transport (e.g., electrical conductivity/resistivity) and mechanical properties. Previous work on transport in stochastic fibrous networks has shown that the transport in dry networks can be characterized using a combined analytic/numerical techniques, whereby networks are constructed using material manufacturing parameters, then connectivity is assessed, and a continuum approach is used to model transport based upon the effective connectivity. Using such simulation techniques, "percolation points" at which transport properties rise or fall dramatically, can be identified, based on the geometry alone. Adaptations of continuum models for conductive fibers in insulating matrices (Sastry, 1994) have shown that transport properties change most rapidly at around 4–5 percent; addition of the

stochastic model (Sastry et al., 1997) has shown that this point must be separately identified for stochastic structures, where the "effective" volume fraction may be considerably different than the nominal volume fraction (i.e., a significant portion of the conductive fibers may be located such that they lie outside of conductive pathways).

In the experiments performed here, it was observed that the response of the higher volume fraction (18% Ni) material was much more sensitive to cycling with respect to electrical conduction than the lower volume fraction material (7% Ni). This points to a more dramatic change in effective conductive network volume in the 18% Ni material upon cycling. There are several possible reasons for this, based on the material behavior. First, there may be a "size effect" at work, whereupon the existence of greater numbers of weaker bonds in the higher volume fraction material causes earlier local failures, which propagate, finally resulting in a proportionally greater loss of effective conductive volume than in the lower volume fraction material. Second, there may be a difference in local failure mechanism in the higher and lower volume fraction materials. Lower volume fraction materials would likely bear more structural load in bending than higher volume fraction materials, and differences in strength between sinter bonds (intersections of fibers) and the fibers themselves (in tension or compression/bending) might play a role. Progressive damage simulations incorporating a variety of these physical failure mechanisms will be part of future work.

In mechanical properties, the response of the lower volume fraction (18% Ni) material was more sensitive to cycling with respect to material modulus than the lower volume fraction material (7% Ni). Modulus reduction in both cases was not severe (10 and 22 percent, respectively). This sensitivity is the reverse of that observed in the resistivity experiments. Local plastic deformation, due to large rotations about sinter bonds, may be playing a role. Such deformation would have little effect on resistivity, but a large effect on mechanical properties, and will be investigated as part of future work.

The cause of the increases observed in peak loads is not immediately apparent, given the loss of connectivity presumably at work in reduction of modulus and increase in resistivity. The primary chemical transformations in the electrode occur in the active material; since no cell failures due to loss of conduction in the electrode, nor reduction in capacity occurred, we postulate that chemical (material) changes in the substrate are unlikely. Strengthening of the bonds, possibly via remaining small deposits of active material, may be the cause of this observation. The negligible mass difference between uncycled and cycled substrates would be explained by small losses of nickel fiber and spheroids due to local failures and handling being balanced by deposits of active material at the fiber-fiber intersections, or synapses. A reasonable failure sequence in this case would be 1) electrochemical cycling causes bond strengthening, possibly via deposits at synapses, 2) electrochemical cycling simultaneously causes loss of connectivity, leading to reduced modulus, and 3) ex situ experiments reveal loss of modulus and increase in resistivity (associated with loss of connectivity) with higher peak stress (associated with higher strength in bond-limited failure).

Crushing of the electrode due to compression in cell packaging may also be a factor in the mechanical response. Future studies will focus on both uncompressed and compressed cells to address this issue. This is a concern in commercial usage of cells, since in most cases compression is currently required in NiMH power packs to both provide contact in the positive plate (to counteract the effects of swelling) and to conform to device packaging constraints.

Guidance in the effect of changing network parameters on network connectivity is the subject of related, ongoing studies in both mechanical response and transport properties. Future work will include validation in NiMH cells under assumed, complex loading conditions, along with studies of in situ transport, incorporating the effect of conductive active material and electrolyte.

Acknowledgments

This work was supported by the Lawrence Berkeley Laboratories, through the Exploratory Research Program of the U.S. Department of Energy, Dr. Albert Landgrebe and Dr. K. Kinoshita, program managers. The authors also gratefully acknowledge support provided by Yardney Technical Products, Pawcatuck, CT, for technical information and materials provided by Mr. Robert Hellen and Mr. Tom Kelly. Materials and materials information provided by Ms. Susan Herczeg of National Standard, and materials and technical assistance provided by Mr. Marshall Muller at Ovonic Battery Company are also gratefully acknowledged.

References

Davolio, G., Da Pieve, A., and Soragni, E., 1990, "On the Mechanical Properties of Nickel Oxide Electrodes," *Proceedings of the Symposium on Nickel Hydroxide Electrodes,* Hollywood, FL.

Ettel, V. A., 1994, "Improving the Pasted Nickel Electrode," *Proceedings, The Eleventh International Seminar on Primary and Secondary Battery Technology.*

Ettel, V. A., Jan., 1993, "Inco's R&D Support for Ni-Based Cells," *Batteries International,* pp. 32–36.

Fritts, D. H., 1981, "Testing the Mechanical Characteristics of Sintered Nickel Battery Plaque and Their Relationship to Nickel Electrode Performance," *Journal of Power Sources,* Vol. 6, pp. 171–184.

Oshitani, M., Takayama, T., Takashima, K., and Tsuji, S., 1986, "A Study on the Swelling of Sintered Nickel Hydroxide Electrode," *Journal of Applied Electrochemistry,* Vol. 16, pp. 403–412.

Sastry, A. M., Cheng, X., and Choi, S. B., 1997, "Transport in Fibrous Battery Electrode Substrates," *Proceedings of the 1997 International Mechanical Engineering Congress & Exposition,* Nov. 16–21, Dallas, TX, MD80, pp. 331–338.

Sastry, A. M., Cheng, X., and Wang, C., 1998, "Mechanics of Stochastic Fibrous Networks," *Journal of Thermoplastic Composite Materials,* Vol. 11, pp. 288–296.

Sastry, A. M., 1994, "Modeling Conductivity of Composite Substrates for Nickel-Metal Hydride Batteries," Sandia Report SAND94-2884.

USABC, 1996, "USABC Electric Vehicle Battery Test Procedures Manual, Revision 2," principal author: Gary Hunt, Idaho National Engineering Laboratory (INEL), U.S. Department of Energy Idaho Field Office, DOE/ID-10479, Rev. 2.